Recent top cross-section measurements with the ATLAS detector

Peter Hansen, University of Copenhagen
On behalf of the ATLAS Collaboration

12’th edition of the LHC Physics Conference, Boston, June 2024

Why measure top cross-sections

ATLAS records up to 30 top quarks per second! Inclusive and differential cross-section measurements offer a unique opportunity

- to test QCD at the m_{top} scale, allowing tests with a precision of a few %.
- to measure basic SM parameters, such as m_{top}, V_{tb}, α_s.
- to constrain the proton PDF's, the top background to BSM processes and BSM EFT contributions to the cross-sections.

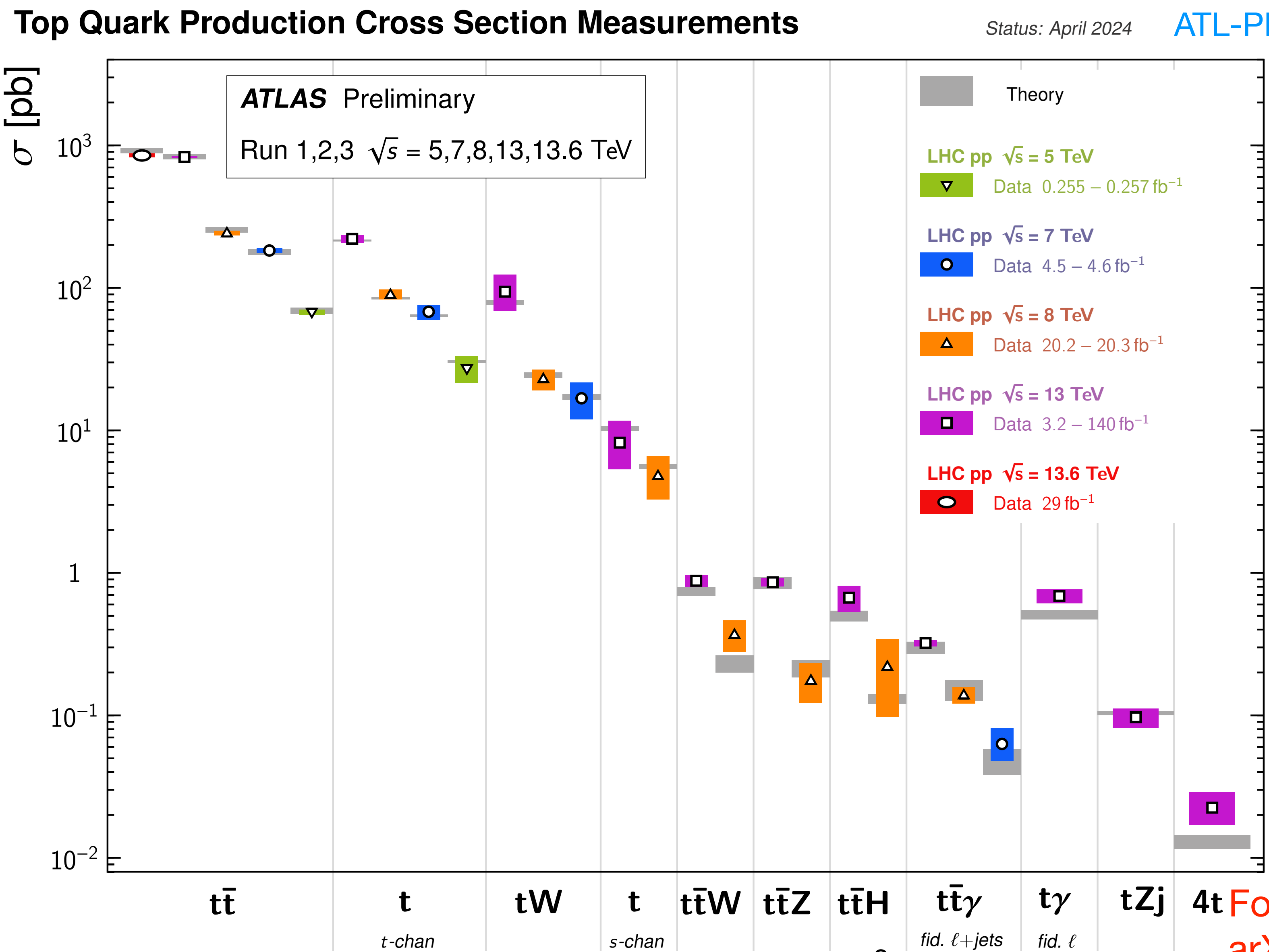

ATL-PHYS-PUB-2024-006

Measurements spanning 5 orders of magnitude.

The most precise is $\sigma_{t\bar{t}}$ at 13 TeV with 1.8% uncertainty.
JHEP 07 (2023) 141

Steep energy dep. due to the high top mass.

This talk focuses on recent $t\bar{t}$ and single-top measurements with the entire Run2 (140 fb^{-1}) or early Run3 samples.

For a comprehensive review see arXiv:2404.106754

Early result from Run3 : $t\bar{t}$ at 13.6 TeV

Phys. Lett. B 848 (2024) 138376,

Tests the $\sqrt{s}$ dep. with the upgraded ATLAS detector using the dilepton channel with 29 fb^{-1}.

Events are counted in a fiducial region, defined roughly to have two opp. sign leptons with p_T>27 GeV and at least one b-jet (in case of $e\mu$), and 66 GeV < m_{ll} <116 GeV (in the case of same-flavor leptons). The $t\bar{t}$ and Z cross-sections, as well as the b-tagging efficiency, are extracted from the event yields in the 0-1-2-bjet cases.

$\sigma_{t\bar{t}} = 850 \pm 3(stat) \pm 18(syst) \pm 20(lumi)$ pb

$R_{t\bar{t}/Z} = 1.145 \pm 0.003(stat) \pm 0.021(syst) \pm 0.002(lumi)$ pb

1.5 and ~1σ, respectively, lower than NNLO prediction (PRL110 (2013) 252004)

where the "syst" is dominated by signal modelling uncertainties

$R_{t\bar{t}/Z}$ prediction is NNLO + NLO-EW

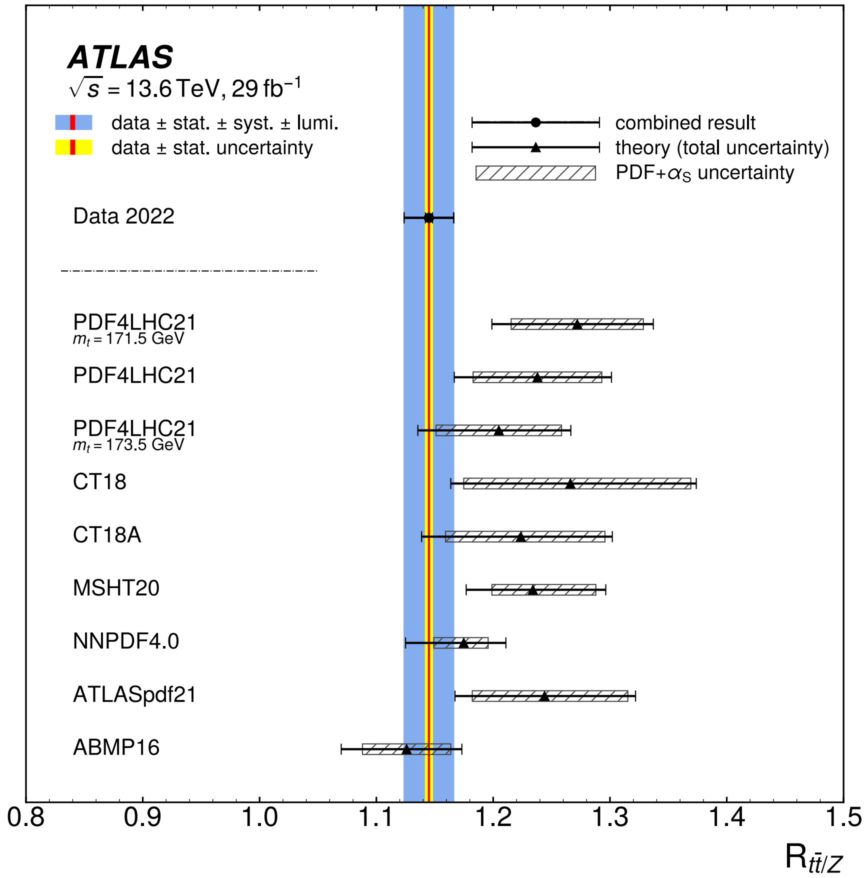

The other extreme in collision energy: 5.02 TeV

JHEP 06 (2023) 138

The inclusive $t\bar{t}$ cross-section was also measured at 5.02 TeV in a low pile-up run in 2017 with 257 pb^{-1}. The result is

$\sigma_{t\bar{t}} = 67.5 \pm 2.7$ pb. (Only 3.9%!)

In excellent agreement with the NNLO prediction

$\sigma^{pred}_{t\bar{t}} = 68.2^{+5.2}_{-5.3}$ pb PRL110 (2013) 252004

The 5.02 TeV measurement constrains the gluon PDF for x>0.05.

In general, the measurements of inclusive $t\bar{t}$ x-sections over a wide range of energies probe the PDF and different production channels spanning an order of magnitude in cross-sections.

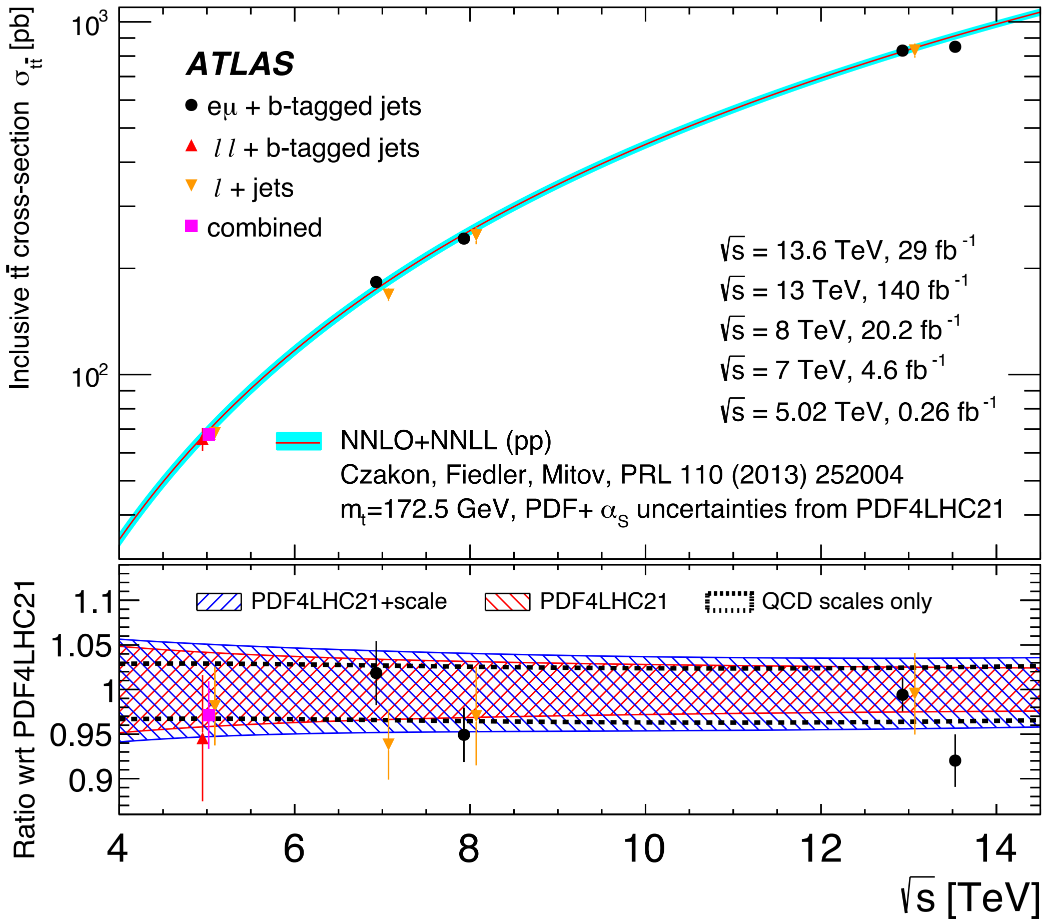

Jets associated with $t\bar{t}$ production, 13 TeV

- Use the lepton + jets (at least 1 b tagged) channel to test modelling of signal and background
- Many kinematical variables formed by the jets from W decay and jets from gluon radiation are studied. Here is the measured $\frac{d\sigma}{dp_T}$ of the W jets, the first radiated jet and the second radiated jet compared with predictions:

ATLAS-CONF-2023-068

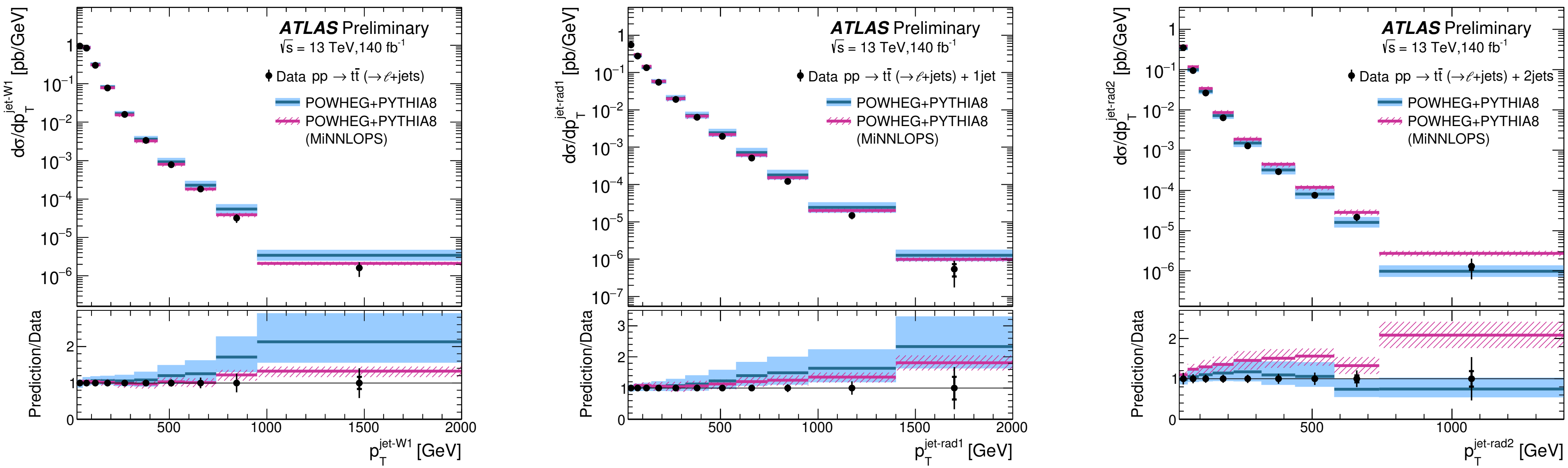

The NNLO generator, MiNNLOPS (JHEP 05 (2020) 143), provides a better description than the NLO generator of the W-jets and the first radiated jet, but not of the second radiated jet.

Jet substructure in $t\bar{t}$ events, 13 TeV

arXiv:2312.03797

New measurement of boosted top-jets with increased precision and detail due to the use of full Run2, both semi-leptonic and all-hadronic channels, and charged particles for substructure.

Select top-jets with $p_T > 350$ GeV (l+jets) and $p_T > 500$ GeV (all-had) using tag & probe.

Normalised differential cross-sections are measured as a function of 8 substructure variables (some separated into different m_{top} and p_T^{top} regions):

- τ_{32}, τ_3, C_3 ("3-bodyness") and D_2, τ_{21} ("2-bodyness")
- $p_T^{d,*}$ (momentum dist), LHA (broadness) and $ECF2$ (energy-energy correlations)

While the absolute cross-sections are known to be overestimated at high p_T by NLO models, the normalised ones are sensitive probes of the parton shower and hadronization aspects of the models.

Jet substructure in $t\bar{t}$ events, 13 TeV

arXiv:2312.03797

- Unfolded to particle level.
- Both reclustered jets (RC) and R=1 jets are considered
- Systematic uncertainties are 2-10%. Largest ones are from parton shower (l+jets) and JES (all-had)

Overall agreement between distributions in data and NLO models. However, Pwg+Py8 is more “3-body” than data in τ_{32}, C_3, τ_3 -especially its FSR up variation - Also $p_T^{d,*}$ is significantly softer in the data than in Pwg+Py8.

Pwg+H7, aMC@NLO+Py8 and Pwg+Py8(FSR down) provide better descriptions of the data.

l+jets

All-had

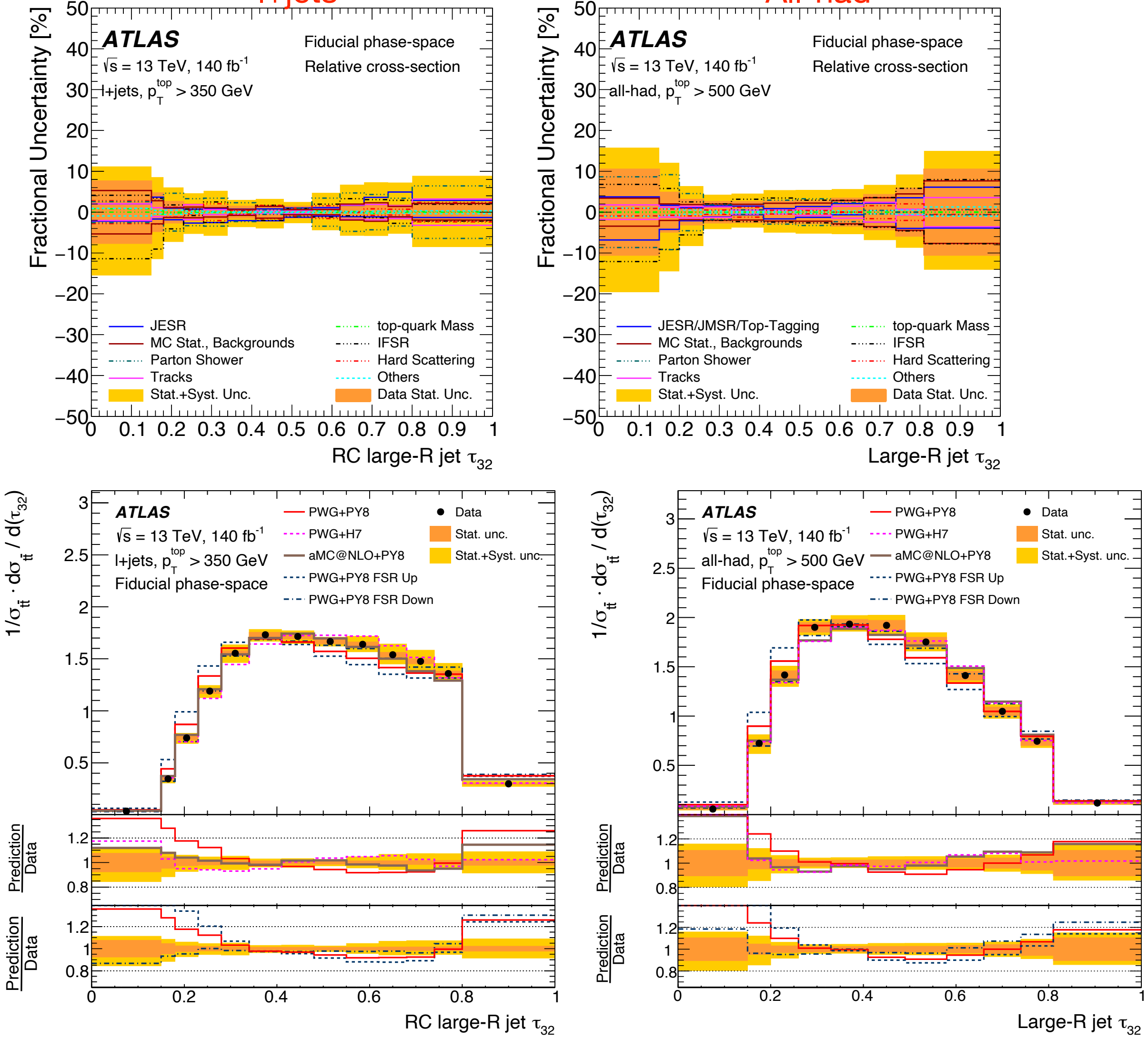

Single top, t-channel, 13 TeV

Select $(bl\nu)j$ events by confining reconstructed objects to two kinematic SR's favoring tq (one for each lepton charge).

The SR's still hold a large background from $t\bar{t}$ and $Wb\bar{b}$, which is further separated from the signal by a NN combination of 17 kinematic variables, including the reconstructed top mass.

The signal cross-section is extracted from a profile likelihood fit to the NN output in the SR and the event yields in several CR's with inverted cuts. The fit is good (P=76%).

Signal and background modelling contribute the largest uncertainties.

JHEP 05 (2024) 305

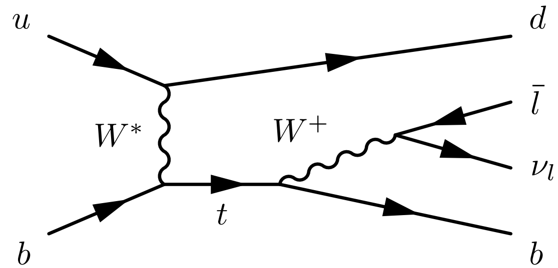

Tests Wtb vertex, u/d PDF

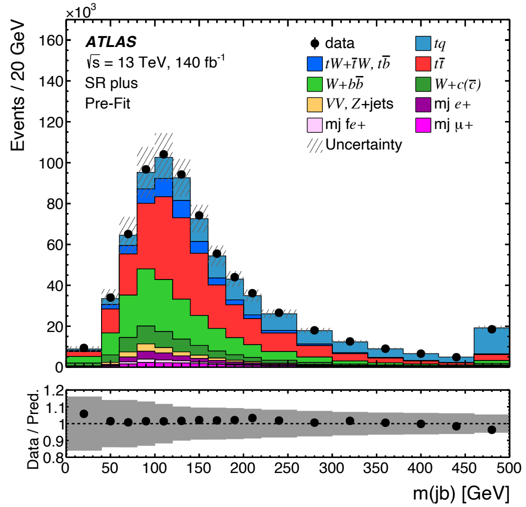

Most sensitive variable m(jb)

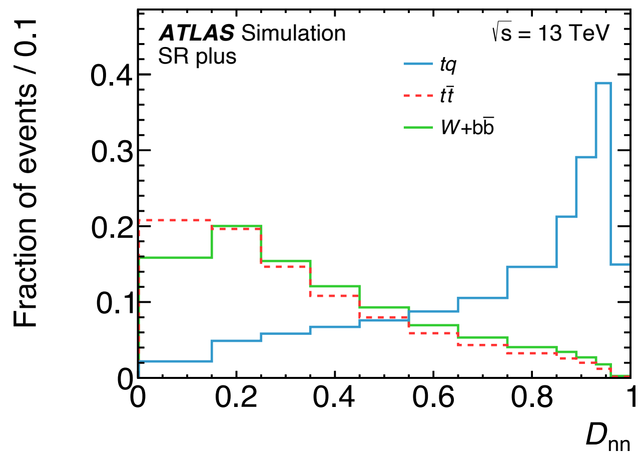

NN output

Single top, t-channel, 13 TeV, results:

$\sigma_{tq} = 137^{+8}_{-8}$ pb and $\sigma_{\bar{t}q} = 84^{+6}_{-5}$ pb

(MCFM 10.1: 134.2 ± 2.2 pb and 80.0 ± 1.8 pb, JHEP 02 (2021)040)

$\sigma(tq + \bar{t}q) = 221 \pm 13$ pb, (MCFM 10.1: 214 ± 2.7 pb)

$$R_t = \sigma(tq)/\sigma(\bar{t}q) = 1.636^{+0.036}_{-0.034}$$

An EFT interpretation finds new limits on a four-quark point interaction :

$$-0.37 < C^{3,1}_{Qq}/\Lambda^2 < 0.06,$$

as well as new limits on an anomalous tH coupling:

$$-0.87 < C^{3}_{\phi Q}/\Lambda^2 < 1.42$$

Assuming $f_{LV} = 1$ and $|V_{tb}| \gg |V_{ts}|, |V_{td}|$, the data give the limit

$$|V_{tb}| > 0.95 \text{ at 95\% conf.}$$

If the assumptions are released, more general limits on $f_{LV}|V_{tq}|$ are set:

JHEP 05 (2024) 305

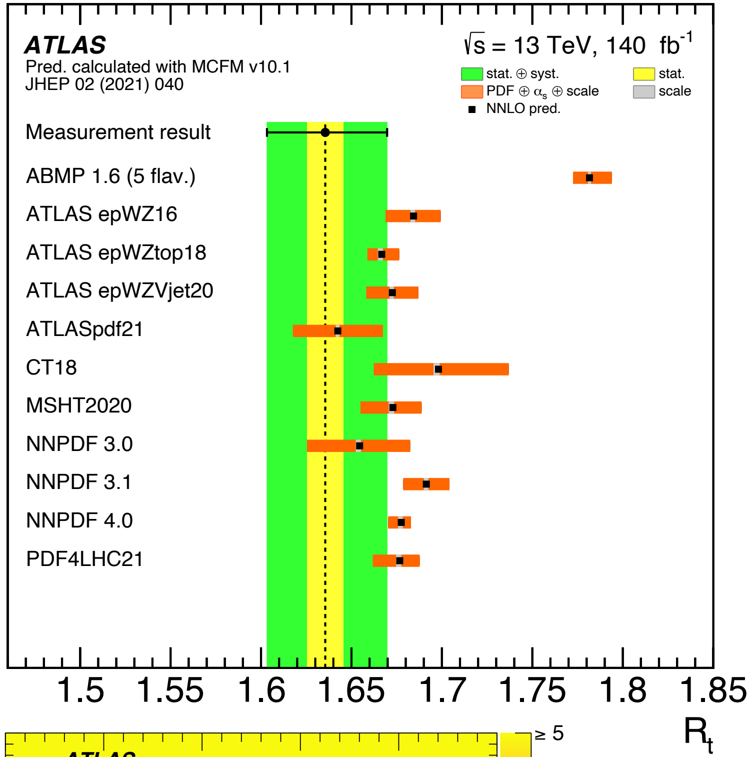

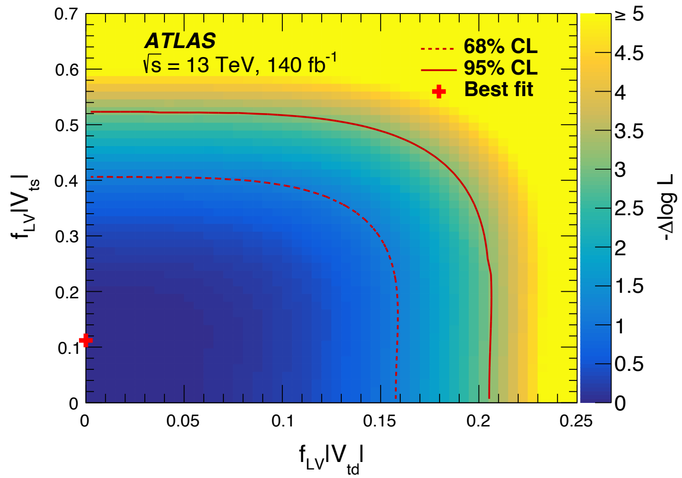

Single top, t-channel, 5.02 TeV

In November 2017 LHC provided 255 pb^{-1} at low pile-up and $\sqrt{s} = 5.02$ TeV. Thus statistics are low.

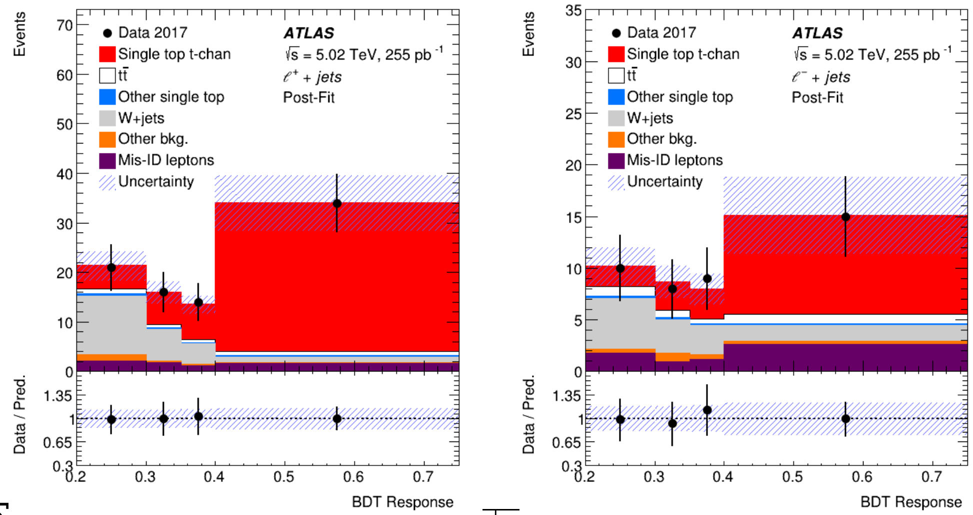

The t-channel cross-section was measured in a similar way, albeit using lower thresholds and a BDT instead of a deep NN, with the results:

$\sigma(tq + \bar{t}q) = 27 \pm 6$ pb,

(MCFM prediction $30.3^{+0.7}_{-0.5}$ pb)

$R_t = \sigma(tq)/\sigma(\bar{t}q) = 2.73^{+1.75}_{-0.89}$

(MCFM prediction $2.03^{+0.06}_{-0.07}$)

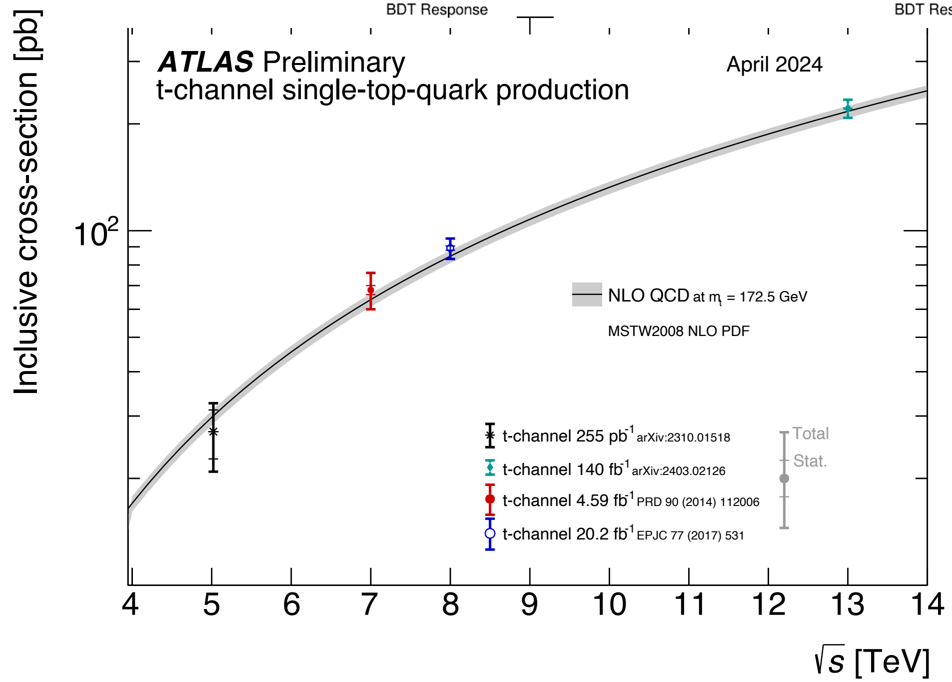

Agreement with NLO QCD and PDF over an order of magnitude in cross-section

Phys.Lett. B 854 (2024) 138726

$t\bar{t}$ in p+Pb collisions, what is the n-modification?

arXiv:2405.05078

2016 p+Pb run, $\sqrt{s_{NN}} = 8.16$ TeV, 165 nb^{-1}

- Sensitive to nPDFs. Needed in order to separate initial state from QGP effects
- Use both di-lepton and l+jets in six SR's, depending on the number of b-jets.
- Profile-likelihood fit of signal yield to the $H_T^{l,jets}$ distribution in all six SR's.

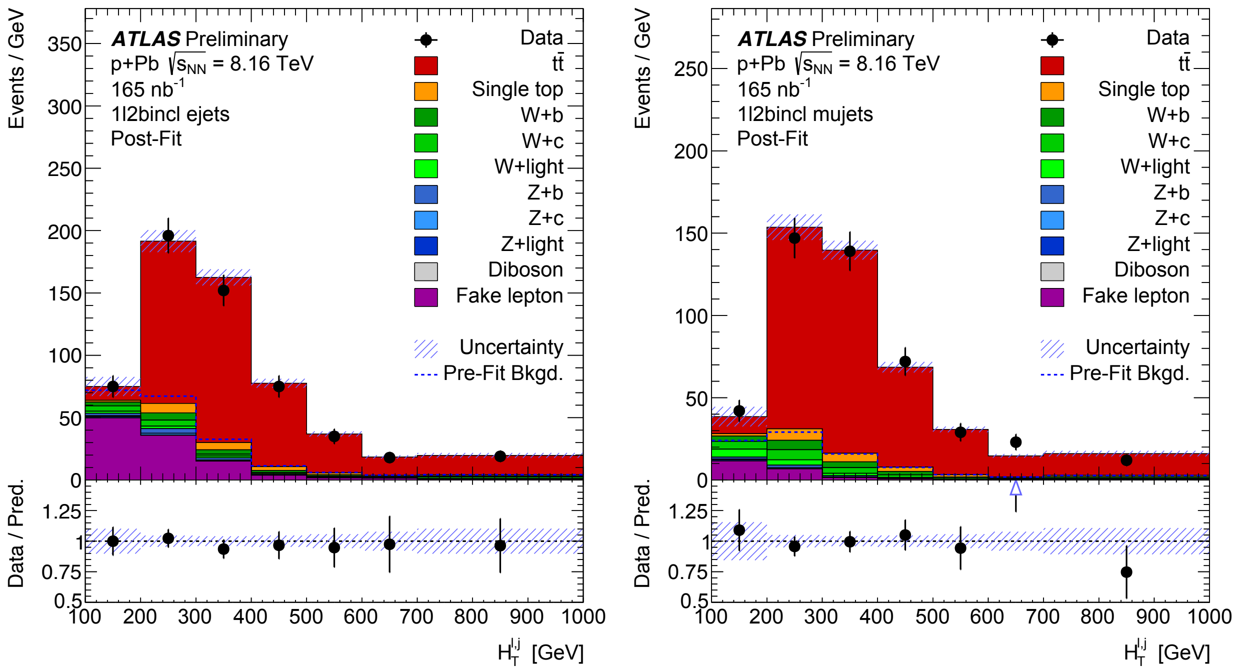

Example: 1 lepton and 2 b-jets :

Dominant pre-fit uncertainties are background normalisations (fake-l, W/Z+jets).

Largest post-fit uncertainties are signal modelling and JES

$t\bar{t}$ in p+Pb collisions, what is the n-modification?

arXiv:2405.05078

$$\mu_{t\bar{t}} = \sigma^{t\bar{t}}_{meas}/(A_{Pb} \times \sigma^{t\bar{t}}_{th}) = 1.04 \pm 0.09$$

>5 sigma observation! First observation of top production in p+A in the di-lepton channel.

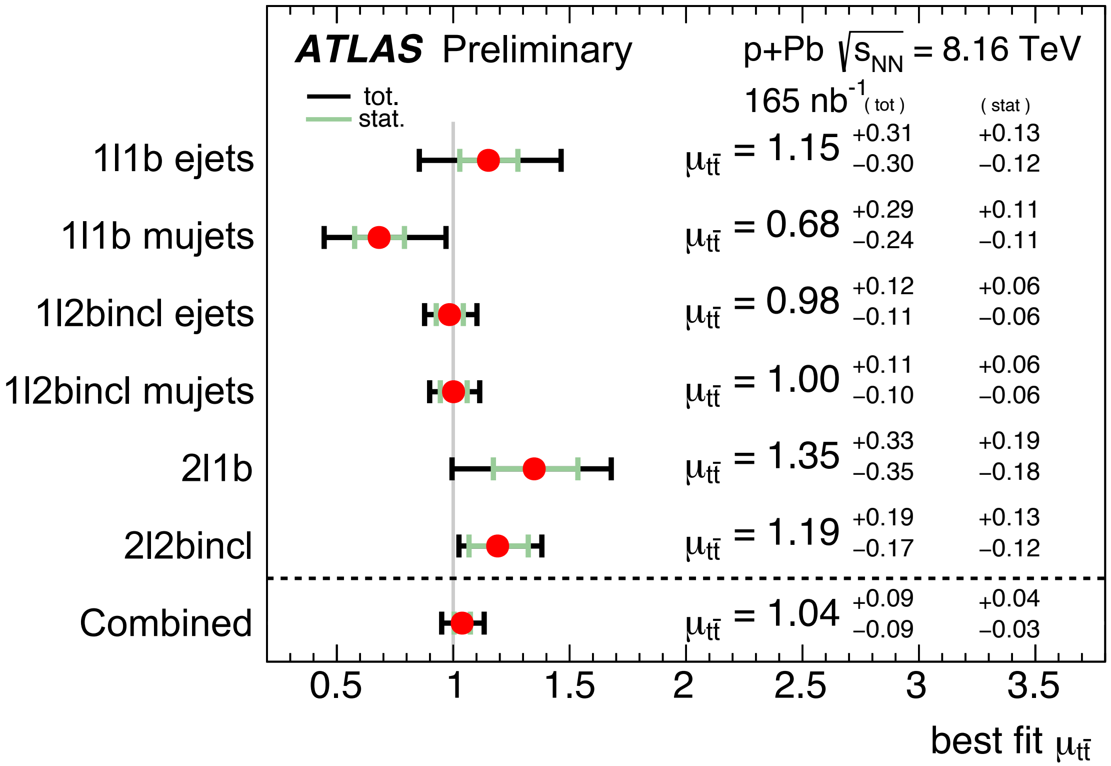

Discriminates between nPDFs

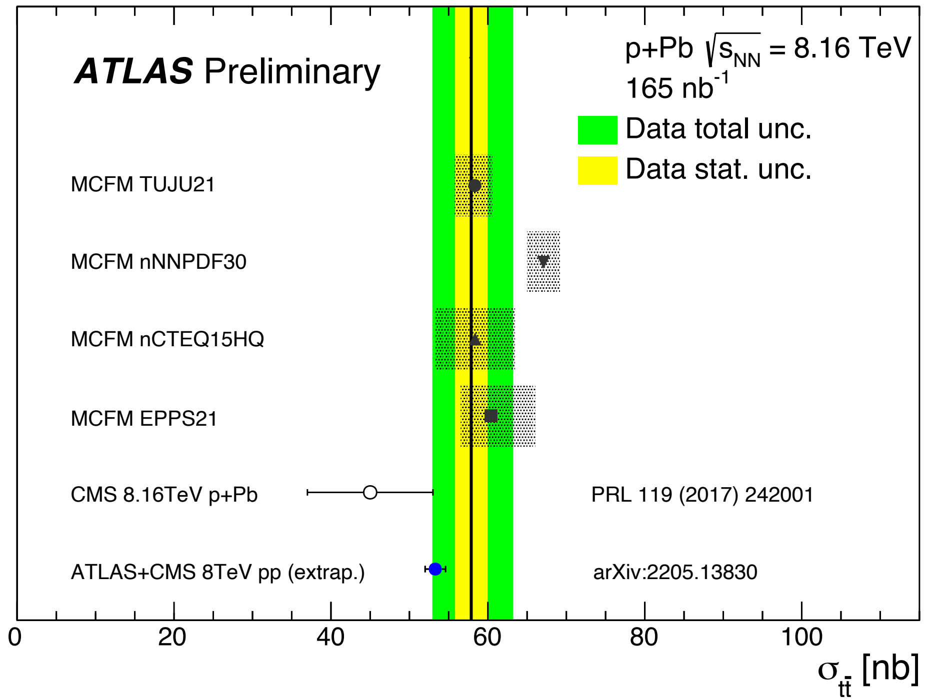

Summary

The large statistics of the full Run2 data sample, together with progress in reducing uncertainties from luminosity, calibration and modelling, has enabled recent ATLAS results on top cross-sections:

- Measurement of inclusive and differential $t\bar{t}$ cross-sections with a precision of 1.8%
- Improved measurements of jets with p_T up to ~2TeV in $t\bar{t}$ events
- Measurements of single top production in the t-channel over a huge $t\bar{t}$ background providing new constraints on the PDFs and the Wtb vertex.

The energy dependence of the cross-sections has been studied using a special run at $\sqrt{s}$ = 5.02 TeV and the first year of Run3 at $\sqrt{s}$ = 13.6 TeV.

In addition, the 2016 p+Pb run has been used to make a 5-sigma observation of $t\bar{t}$ production in p+Pb collisions.

Further progress will come from the Run3 data and in particular from ongoing efforts in QCD modelling aiming to match better the experimental precision.

THANK YOU!

Backup slides

t-tbar and single top

Top Quark Production Cross Section Measurements

Status: April 2024

ATLAS Preliminary

Run 1,2,3 $\sqrt{s}$ = 5, 7, 8, 13, 13.6 TeV

Model	E_{CM} [TeV]	$\int\mathcal{L}\,dt[fb^{-1}]$	Measurement	Theory	Reference
$t\bar{t}$	13.6	29.0 fb^{-1}	$\sigma = 850 \pm 3 \pm 27$ pb	$\sigma = 924 + 32 - 40$ pb (top++ NNLO+NNLL)	PLB 848 (2024) 138376
$t\bar{t}$	13	140 fb^{-1}	$\sigma = 829 \pm 1 \pm 15.4$ pb	$\sigma = 834 + 29 - 37$ pb (top++ NNLO+NNLL)	JHEP 07 (2023) 141
$t\bar{t}$	8	20.2 fb^{-1}	$\sigma = 242.9 \pm 1.7 \pm 8.6$ pb	$\sigma = 256 + 10.4 - 12$ pb (top++ NNLO+NNLL)	EPJC 74 (2014) 3109
$t\bar{t}$	7	4.6 fb^{-1}	$\sigma = 182.9 \pm 3.1 \pm 6.4$ pb	$\sigma = 179.6 + 7.8 - 8.7$ pb (top++ NNLO+NNLL)	EPJC 74: 3109 (2014)
$t\bar{t}$	5	0.3 fb^{-1}	$\sigma = 67.5 \pm 0.9 \pm 2.6$ pb	$\sigma = 69.5 + 3.5 - 3.7$ pb (top++ NNLO+NNLL)	JHEP 06 (2023) 138
t_{t-chan}	13	140 fb^{-1}	$\sigma = 221 \pm 1 \pm 13$ pb	$\sigma = 214.2 + 4.1 - 2.6$ pb (MCFM (NNLO))	arXiv:2403.02126
t_{t-chan}	8	20.3 fb^{-1}	$\sigma = 89.6 \pm 1.7 + 7.2 - 6.4$ pb	$\sigma = 84.3 + 1.7 - 1.2$ pb (MCFM (NNLO))	EPJC 77 (2017) 531
t_{t-chan}	7	4.6 fb^{-1}	$\sigma = 68 \pm 2 \pm 8$ pb	$\sigma = 63.7 + 1.4 - 0.8$ pb (MCFM (NNLO))	PRD 90, 112006 (2014)
t_{t-chan}	5	0.3 fb^{-1}	$\sigma = 27.1 + 4.4 - 4.1 + 4.4 - 3.7$ pb	$\sigma = 30.3 + 0.7 - 0.5$ pb (MCFM (NNLO))	arXiv:2310.01518
tW	13	3.2 fb^{-1}	$\sigma = 94 \pm 10 + 28 - 23$ pb	$\sigma = 79.3 + 2.9 - 2.8$ pb (aNNLO+aN3LL)	JHEP 01 (2018) 63
tW	8	20.3 fb^{-1}	$\sigma = 23 \pm 1.3 + 3.4 - 3.7$ pb	$\sigma = 24.4 + 1.1 - 1$ pb (aNNLO+aN3LL)	JHEP 01, 064 (2016)
tW	7	2.0 fb^{-1}	$\sigma = 16.8 \pm 2.9 \pm 3.9$ pb	$\sigma = 17.1 \pm 0.8$ pb (aNNLO+aN3LL)	PLB 716, 142-159 (2012)
t_{s-chan}	13	139 fb^{-1}	$\sigma = 8.2 \pm 0.6 + 3.4 - 2.8$ pb	$\sigma = 10.32 + 0.4 - 0.36$ pb (Hathor (NLO))	JHEP 06 (2023) 191
t_{s-chan}	8	20.3 fb^{-1}	$\sigma = 4.8 \pm 0.8 + 1.6 - 1.3$ pb	$\sigma = 5.61 \pm 0.22$ pb (NLO+NNL)	PLB 756, 228-246 (2016)

13 TeV differential x-sections in e-mu channel

JHEP 07 (2023) 141

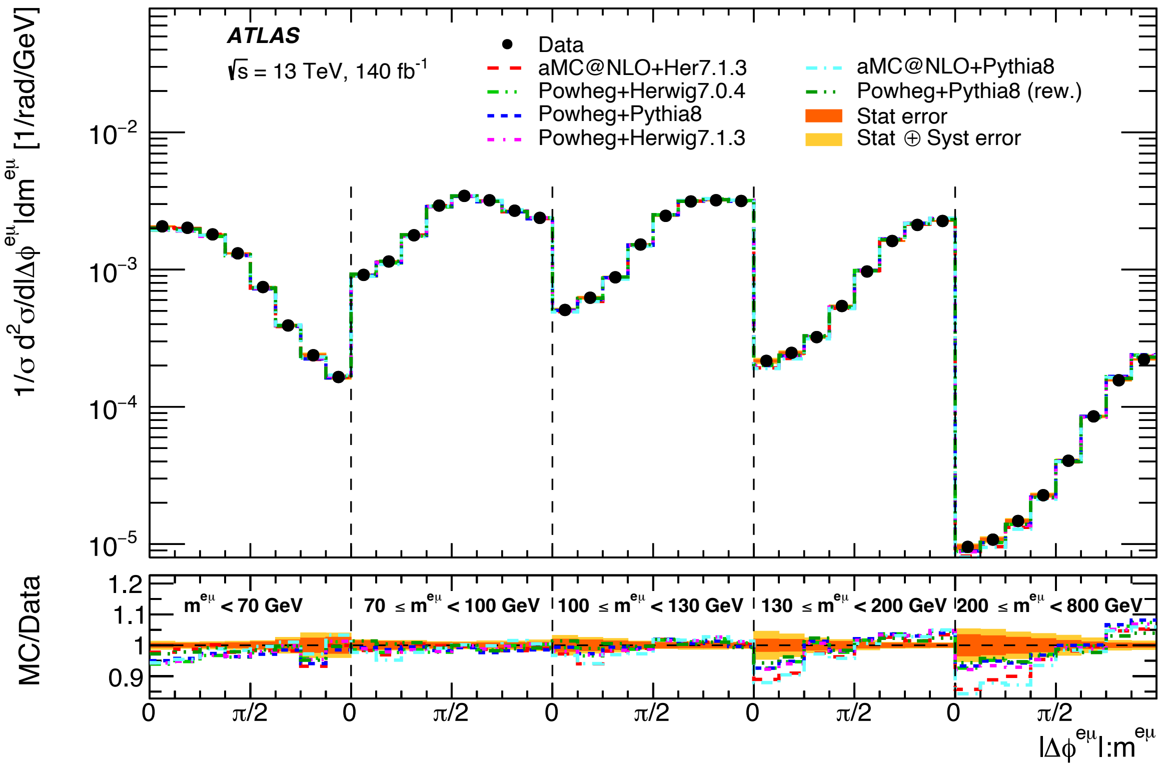

- diff. x-sections as functions of lepton kinematic variables.
- Single and double. Use 140 fb^{-1}.
- Precision 1-2% in normalised spectra
- Modelling, such as Wt background, dominates uncertainties here.
- $\sigma_{t\bar{t}} = 829 \pm 1(stat) \pm 13(syst) \pm 8(lumi) \pm 2(Eb) pb$

1.8% precision! Reduction due to advances in luminosity uncertainty: Eur.Phys.J.C83(2023)982

While the inclusive cross-section is in excellent agreement with the NNLO prediction, no NLO model agrees with all the differential x-sections . The discrepancies are reduced if the models are reweighed to reproduce the NNLO p_T^{top} prediction. (arXiv:2105.03877)

Single top, s-channel

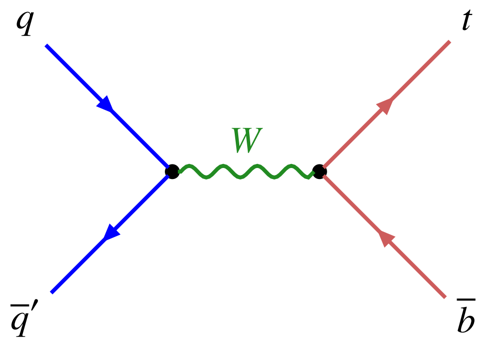

13 GeV , 139 fb^{-1} (JHEP 06 (2023) 191)

The huge $t\bar{t}$ background is controlled via a discriminant $P(schan\,|\,X)$ obtained via Bayes theorem from $P(X, proc) = \int d\Phi \frac{1}{\sigma_{proc}} \frac{d\sigma_{proc}}{d\Phi} T(X\,|\,\Phi)$, where T is a transfer function between parton kinematics Φ and detector level observables X. From a fit to this discriminant in the SR (one lepton, two b-jets, ETmiss), ATLAS finds a 3.3σ signal significance and a x-section of:

$\sigma_{s-chan} = 8.2^{+3.2}_{-2.9}$ pb. (Prediction $10.32^{+0.40}_{-0.36}$, Comput.Phys.Commun.191(2015)74)

$t\bar{t}$ 13.6 TeV, 29 fb^{-1}

Phys. Lett. B 848 (2024) 138376,

Category		Uncertainty [%]		
		$\sigma_{t\bar{t}}$	$\sigma^{\text{fid.}}_{Z\to\ell\ell}$	$R_{t\bar{t}/Z}$
$t\bar{t}$	$t\bar{t}$ parton shower/hadronisation	0.9	< 0.2	0.9
	$t\bar{t}$ scale variations	0.4	< 0.2	0.4
	$t\bar{t}$ normalisation	-	< 0.2	-
	Top quark p_{T} reweighting	0.6	< 0.2	0.6
Z	Z scale variations	< 0.2	0.4	0.3
Bkg.	Single top modelling	0.6	< 0.2	0.6
	Diboson modelling	< 0.2	< 0.2	0.2
	$t\bar{t}V$ modelling	< 0.2	< 0.2	< 0.2
	Fake and non-prompt leptons	0.6	< 0.2	0.6
Lept.	Electron reconstruction	1.2	1.0	0.4
	Muon reconstruction	1.4	1.4	0.3
	Lepton trigger	0.4	0.4	0.4
Jets/tagging	Jet reconstruction	0.4	-	0.4
	Flavour tagging	0.4	-	0.3
	PDFs	0.5	< 0.2	0.5
	Pileup	0.7	0.8	< 0.2
	Luminosity	2.3	2.2	0.3
	Systematic uncertainty	3.2	2.8	1.8
	Statistical uncertainty	0.3	0.02	0.3
	Total uncertainty	3.2	2.8	1.9

$t\bar{t}$ 5.02 TeV, 257 pb^{-1}

JHEP 06 (2023) 138

Category	$\delta\sigma_{t\bar{t}}$ [%] Dilepton	Single lepton	Combination
$t\bar{t}$ generator†	1.2	1.0	0.8
$t\bar{t}$ parton-shower/hadronisation*,†	0.3	0.9	0.7
$t\bar{t}$ h_{damp} and scale variations†	1.0	1.1	0.8
$t\bar{t}$ parton distribution functions†	0.2	0.2	0.2
Single-top background	1.1	0.8	0.6
W/Z + jets background*	0.8	2.4	1.8
Diboson background	0.3	0.1	< 0.1
Misidentified leptons*	0.7	0.3	0.3
Electron identification/isolation	0.8	1.2	0.8
Electron energy scale/resolution	0.1	0.1	< 0.1
Muon identification/isolation	0.6	0.2	0.3
Muon momentum scale/resolution	0.1	0.1	0.1
Lepton-trigger efficiency	0.2	0.9	0.7
Jet-energy scale/resolution	0.1	1.1	0.8
$\sqrt{s} = 5.02$ TeV JES correction	0.1	0.6	0.5
Jet-vertex tagging	< 0.1	0.2	0.2
Flavour tagging	0.1	1.1	0.8
$E_{\text{T}}^{\text{miss}}$	0.1	0.4	0.3
Simulation statistical uncertainty*	0.2	0.6	0.5
Data statistical uncertainty*	6.8	1.3	1.3
Total systematic uncertainty	2.5	4.2	3.4
Integrated luminosity	1.8	1.6	1.6
Beam energy	0.3	0.3	0.3
Total uncertainty	7.5	4.5	3.9

$t\bar{t}$+ jets, 13 TeV, 140 fb^{-1}

ATLAS-CONF-2023-068

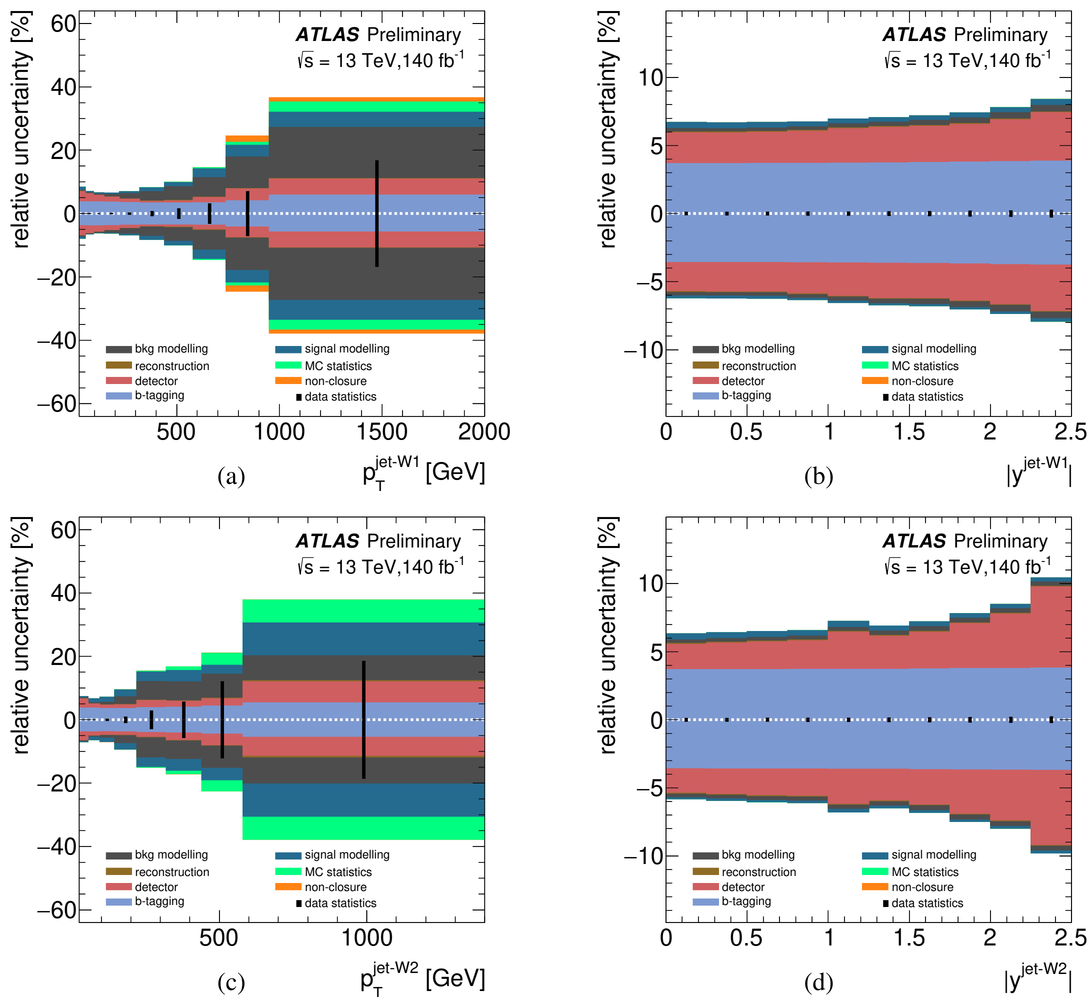

jet substructure in t-tbar events, 13 TeV, 140 fb^{-1}

arXiv:2312.03797

Observable	PWG+PY8		PWG+H7		aMC@NLO+PY8		PWG+PY8(FSR Up)		PWG+PY8(FSR Down)	
	χ^2/NDF	p-value	χ^2/NDF	p-value	χ^2/NDF	p-value	χ^2/NDF	p-value	χ^2/NDF	p-value
τ_{32}	54/12	<0.01	19/12	0.09	15/12	0.24	165/12	<0.01	40/12	<0.01
τ_{21}	14/14	0.41	7/14	0.92	16/14	0.32	42/14	<0.01	8/14	0.91
τ_3	36/11	<0.01	42/11	<0.01	14/11	0.23	130/11	<0.01	23/11	0.02
$ECF2$	25/18	0.13	13/18	0.78	15/18	0.69	31/18	0.03	24/18	0.14
D_2	20/16	0.20	17/16	0.39	20/16	0.20	37/16	<0.01	15/16	0.49
C_3	11/14	0.65	6/14	0.97	3/14	1.00	35/14	<0.01	3/14	1.00
$p_{\mathrm{T}}^{\mathrm{d},*}$	27/12	<0.01	10/12	0.58	11/12	0.53	56/12	<0.01	24/12	0.02
LHA	14/17	0.65	9/17	0.92	20/17	0.29	14/17	0.69	19/17	0.32
D_2 vs. m^{top}	61/42	0.03	62/42	0.02	59/42	0.05	118/42	<0.01	44/42	0.37
D_2 vs. $p_{\mathrm{T}}^{\mathrm{top}}$	71/56	0.08	68/56	0.13	70/56	0.11	107/56	<0.01	93/56	<0.01
τ_{32} vs. m^{top}	153/42	<0.01	72/42	<0.01	56/42	0.07	413/42	<0.01	77/42	<0.01
τ_{32} vs. $p_{\mathrm{T}}^{\mathrm{top}}$	153/50	<0.01	103/50	<0.01	57/50	0.23	360/50	<0.01	114/50	<0.01

Table 3: χ^2 and p-values quantifying the level of agreement between the unfolded spectra in the all-hadronic channel and several suitably normalized NLO+PS predictions. PWG+PY8 corresponds to the Powheg+Pythia sample and PWG+H7 to the Powheg+Herwig sample.

Observable	PWG+PY8		PWG+H7		aMC@NLO+PY8		PWG+PY8(FSR Up)		PWG+PY8(FSR Down)	
	χ^2/NDF	p-value	χ^2/NDF	p-value	χ^2/NDF	p-value	χ^2/NDF	p-value	χ^2/NDF	p-value
τ_{32}	24/10	<0.01	14/10	0.20	9/10	0.52	61/10	<0.01	6/10	0.82
τ_{21}	7/10	0.75	6/10	0.80	6/10	0.80	11/10	0.36	6/10	0.84
τ_3	29/7	<0.01	17/7	0.02	10/7	0.17	58/7	<0.01	8/7	0.29
$ECF2$	17/11	0.10	12/11	0.39	14/11	0.26	20/11	0.05	15/11	0.19
D_2	11/12	0.55	8/12	0.82	8/12	0.76	14/12	0.27	7/12	0.88
C_3	29/8	<0.01	21/8	<0.01	13/8	0.13	57/8	<0.01	10/8	0.28
$p_{\mathrm{T}}^{\mathrm{d},*}$	21/9	0.01	6/9	0.78	10/9	0.35	35/9	<0.01	8/9	0.54
LHA	12/12	0.49	9/12	0.74	12/12	0.46	12/12	0.43	11/12	0.53
D_2 vs. m^{top}	22/32	0.91	27/32	0.73	20/32	0.95	28/32	0.67	19/32	0.96
D_2 vs. $p_{\mathrm{T}}^{\mathrm{top}}$	29/43	0.96	26/43	0.98	28/43	0.96	32/43	0.88	26/43	0.98
τ_{32} vs. m^{top}	30/27	0.31	21/27	0.79	15/27	0.97	69/27	<0.01	11/27	1.00
τ_{32} vs. $p_{\mathrm{T}}^{\mathrm{top}}$	49/37	0.08	36/37	0.53	34/37	0.63	94/37	<0.01	30/37	0.79